Pharmaceutical Research, Vol. 26, No. 7, July 2009 (© 2009)
DOI: 10.1007/s11095-009-9888-0

Research Paper

Nanoparticle Coated Submicron Emulsions: Sustained *In-vitro* Release and Improved Dermal Delivery of All-*trans*-retinol

Nasrin Ghouchi Eskandar,[1] Spomenka Simovic,[1] and Clive A. Prestidge[1,2]

Received December 1, 2008; accepted April 2, 2009; published online April 22, 2009

Purpose. The aim of this research is to investigate the dermal delivery of all-*trans*-retinol from nanoparticle-coated submicron oil-in-water emulsions as a function of the initial emulsifier type, the loading phase of nanoparticles, and the interfacial structure of nanoparticle layers.
Methods. The interfacial structure of emulsions was characterized using freeze-fracture-SEM. *In-vitro* release and skin penetration of all-*trans*-retinol were studied using Franz diffusion cells with cellulose acetate membrane, and excised porcine skin. The distribution profile was obtained by horizontal sectioning of the skin using microtome-cryostat and HPLC assay.
Results. The steady-state flux of all-*trans*-retinol from silica-coated lecithin emulsions was decreased (up to 90%) and was highly dependent on the initial loading phase of nanoparticles; incorporation from the aqueous phase provided more pronounced sustained release. For oleylamine emulsions, sustained release effect was not affected by initial location of nanoparticles. The skin retention significantly ($p \leq 0.05$) increased and was higher for positive oleylamine-stabilised droplets. All-*trans*-retinol was mainly localized in the epidermis with deeper distribution to viable skin layers in the presence of nanoparticles, yet negligible permeation (~1% of topically applied dose) through full-thickness skin.
Conclusions. Sustained release and targeted dermal delivery of all-*trans*-retinol from oil-in-water emulsions by inclusion of silica nanoparticles is demonstrated.

KEY WORDS: all-*trans*-retinol; *in-vitro* release; silica nanoparticles; skin penetration/permeation; submicron emulsion.

INTRODUCTION

Retinoids (natural and synthetic derivatives of retinol) are a homologous series of lipophilic compounds with great importance in modern therapeutic and cosmetic dermatological preparations (1). Vitamin A is prominent for promotion of general growth; the maintenance of visual function; the regulation of the epithelial tissue proliferation and differentiation; and reproduction (2). Among retinoids, retinol and retinyl palmitate can induce epidermis thickening and stratum corneum thinning with less skin irritation and toxicity compared to retinoic acid (3).

The formulation of all-*trans*-retinol into dermal delivery systems is challenging due to poor water solubility (4) and various instability pathways such as isomerisation to *cis* isomers with reduced activity, molecular fragmentation, and photochemical and chemical oxidation (5). Furthermore, oil-in-water emulsions, which are generally the formulations of choice for dermatological products, undergo physical instability after application on the skin surface due to the evaporation of water and release of an oily phase comprising the lipophilic active agent. This phenomenon as well as the lipophilic nature of all-*trans*-retinol, incorporated into the oil phase, limits it's skin absorption from emulsions (6,7).

Liposomes (8), multiple emulsions (9), polymeric systems (10), solid lipid nanoparticles (11,12), egg albumin microspheres (13), and collagen microparticles (14) have been investigated as dermal delivery vehicles of retinoids; however significant challenges remain in the development of highly stable formulations which can deliver sufficient doses of all-*trans*-retinol to the target skin layers.

Simovic and Prestidge (15) showed that nanoparticle layers significantly influence the release kinetics of a model lipophilic drug (di-butyl-phthalate (DBP)) from polydimethylsiloxane oil-in-water emulsions; either sustained or enhanced release can be achieved depending on the nanoparticle layer structure and drug loading level. Nanoparticle layers can be engineered to facilitate a range of release behaviours and offer great potential in the delivery of poorly soluble drugs.

Particle stabilised emulsions have been extensively studied in terms of stabilisation mechanisms (16,17), synergy with common emulsifiers (18,19), and interfacial properties (20,21). However, few reports have focused on their carrier properties as dermal delivery vehicles, e.g. penetration and

[1] Ian Wark Research Institute, ARC Special Research Centre for Particle and Material Interfaces, University of South Australia, Adelaide, South Australia 5095, Australia.
[2] To whom correspondence should be addressed. (e-mail: clive.prestidge@unisa.edu.au)

targeting skin layers. The aim of this research was to investigate the influence of nanoparticle coating of submicron oil-in-water emulsion droplets on the *in-vitro* release and dermal delivery characteristics, with particular emphasis on potential controlled release and targeted skin delivery of all-*trans*-retinol. Medium-chain triglyceride oil-in-water emulsions have been stabilised with mixed interfacial layers composed of lecithin or oleylamine and hydrophilic silica nanoparticles using a simple cold high pressure homogenization technique. Significant improvement in the emulsification efficiency and physical stability of submicron triglyceride oil-in-water emulsions has been reported in our previous work (22). In the current study, we report the improved dermal delivery of all-*trans*-retinol and correlation with interfacial and physicochemical properties of the emulsion carriers.

MATERIALS AND METHODS

Materials

High-purity (Milli-Q) water was used throughout the study (pH=6.5±0.5). Miglyol®812 (Hamilton Laboratories, Australia) was used as the oil vehicle and corresponded to medium chain triglycerides (MCT oil) consisting of semisynthetic triglycerides with >95% octanoic and decanoic acid as fatty acids. Soybean lecithin (BDH) containing >94% phosphatidylcholine and less than 2% triglycerides, and oleylamine (Aldrich) with >98% primary amine were used as received. Fumed silica nanoparticles (Aerosil®380, Degussa, Germany) are reported to have a primary average diameter of 7 nm, BET surface area of 380±30 $m^2\ g^{-1}$, and 2.5 Si–OH groups per nm^2 (determined from Li–Al hydride method) (23). Contact angles estimated from enthalpy of immersion data are reported to be 14° (water/air) and 0° (toluene/water) (24). Synthetic crystalline all-*trans*-retinol (≥95% HPLC) was purchased from Sigma. The solvents were acetonitrile (LiChrosolv®, Merck), acetone (LiChrosolv®, Merck), ethanol absolute, Multisolvent® HPLC grade ACS ISO UV-VIS (Scharlau, Spain), orthophosphoric acid (HiPerSolv®, BDH), and isopropyl myristate (≥98.0% GC, Fluka).

Methods

Emulsion Preparation

Lecithin (0.6 wt.%) or oleylamine (1.0 wt.% with regard to whole emulsion) were added to MCT oil and stirred for 2 h for complete mixing. All-*trans*-retinol (0.05 wt.%) was then added and the oil phase was stirred until complete dissolution and formation of a clear phase. All-*trans*-retinol is a Class II, Type C drug i.e. it is predominantly oil-soluble (solubility in Miglyol®812: 26%) and uncharged (pK_a=14.09±0.10) at the formulation pH of 5.5–6.5 (25,26).

When incorporated from the oil phase, silica nanoparticles were added to the oil phase and the mixture was sonicated for 2 h to achieve the desired size distribution (50±5 nm). For incorporation of nanoparticles from the water phase, aqueous silica dispersion (1.0 wt.%, 50±5 nm) was added to the water phase of the emulsion to achieve the desired concentration of silica. After addition of the aqueous phase to the oil phase, the premix is formed which was then homogenised by a high pressure homogeniser (EmulsiFlex-C5, Avestin® Inc.) at 750±250 bar for five cycles to form the final emulsion. With the aforementioned method, oil-in-water emulsions with 10% oil phase volume fraction and submicron size droplets were prepared. To avoid the effect of UV light, high temperature and oxygen during the preparation process, the samples were prepared in amber glass vials under nitrogen gas and using an ice bath.

Physicochemical and Interfacial Emulsion Characterization

Size, polydispersity index (the width of particle size distribution), and the zeta potential of emulsions in the absence and presence of nanoparticles were measured with dynamic light scattering (Zetasizer Nano ZS, Malvern Instruments, Ltd.). Refractive index values of water (1.33) as the emulsion continuous phase, MCT oil for the control emulsion (1.45) and silica (1.46) were used in the size measurements. Emulsions were diluted 1:100 in MilliQ water and measured in the specified cuvettes at 20±0.5°C. A freeze-fracture scanning electron microscope (Philips XL 30 FEG-SEM with an Oxford CT 1500 cryo transfer system) was used to characterize the interfacial structure of control and silica-coated emulsions. The process contained emulsion cryofixation, fracturing, etching, platinum coating, and imaging. Emulsion samples were injected into a "split" brass tube mounted on the cryo transfer specimen holder. The "split" brass tube consisted of two brass cylinders (ID 1 mm, OD 1.5 mm, L 3.5 mm) lightly glued together with superglue (cyanoacrylate). The emulsions were cryofixed by plunging the "split" brass cylinder and cryo transfer specimen holder into a liquid nitrogen-solid nitrogen slush (−196°C). After cryofixation, the specimen was transferred under vacuum to the specimen exchange chamber of the cryo transfer system (−150°C and 10^{-6} Torr) and the "split" brass tube was broken with a single scalpel blade precooled to −150°C. The surface ice was removed during a sublimation step by increasing the temperature to 95°C for 2 min with great care to avoid droplet disintegration. The fractured and etched sample was then sputter-coated with platinum (~2 nm) for conductivity prior to SEM imaging. X-ray microanalysis (EDAX Genesis V5.21) was used for elemental analysis of the selected areas of the images (21).

Quantitative Assay of All-trans-retinol

A pure authentic all-*trans*-retinol standard has a maximum UV absorption at 325 nm (27). No shift in the absorbance maximum and the UV spectrum was observed for all-*trans*-retinol in different solvent systems (ethanol, hexane/dioxane, methanol/water) (28). High performance liquid chromatography (HPLC) analysis was conducted under isocratic conditions at ambient temperature using a reversed phase column (LiChrospher RP Select B 5 μ, 250×4.6 mm ID, Alltech); the method was adopted from Jenning and Gohla (26). The system consisted of an isocratic pump (Shimadzu LC-6A), auto-injector (Shimadzu SIL-10A), and a UV spectrophotometric detector (Shimadzu SPD-6A). HPLC data were processed and analysed using a chromatopac (Shimadzu C-R3A). Acetonitrile/water (80:20) plus 0.1 vol.% orthophosphoric acid constituted the mobile phase and the

flow rate was adjusted to 1 mL min^{-1}. UV detection was performed at 325 nm for a run time of 15 min and the retention time of all-*trans*-retinol was ~12 min.

Calibration curves for all-*trans*-retinol were constructed in acetone and ethanol/water (50:50) using an external standard method. The stock solution of all-trans-retinol in acetone or ethanol/water with concentration of 25 μg mL^{-1} was prepared in an amber glass volumetric flask and diluted to achieve calibration solutions. Linear calibration curves (R^2 >0.99) were plotted for the integrated peak areas as a function of all-trans-retinol concentrations ranging from 0.05 to 1.5 μg mL^{-1} without addition of an internal standard due to the high specificity and reproducibility of the assay. The limit of detection (LOD: signal-to-noise ratio of 3) of all-*trans*-retinol in acetone and ethanol/water was determined to be 100 and 20 ng mL^{-1}, respectively. The limit of quantification (LOQ: signal-to-noise ratio of 10) was 250 and 50 ng mL^{-1}. The intra-day precision was expressed by relative standard deviation (RSD) of six replicate injections on the same day and was 0.47%, 0.66%, and 0.69% for the lowest, middle and highest calibration points. Due to the instability of all-*trans*-retinol, all samples were prepared fresh and the inter-day precision was not performed. The accuracy for the aforementioned samples was 100.3%, 96.6%, and 107.4% respectively.

In-vitro Active Release

In-vitro release of vitamin A from bare and nanoparticle-coated emulsions was studied for 72 h using vertical one-chamber Franz diffusion cells (PermeGear Inc., USA); these are standard jacketed cells with an orifice diameter of 9.0± 0.5 mm, a 5 mL receptor volume and an effective diffusion area of 0.64±0.03 cm^2. The receptor compartment contained a 50% hydroalcoholic (H_2O/EtOH) solution to allow the establishment of sink conditions (Due to the fact that all-*trans*-retinol is soluble in ethanol, sink conditions was provided by using ethanol/water 50:50 vol.% as the receptor phase. The highest concentration of all-trans-retinol in the receptor phase was 1.72 μg mL^{-1} and this concentration compared to the solubility definition of The United States Pharmacopoeia (Soluble: 10–30 parts of solvent is required for 1 part of solute) is very low, i.e. less than 10% of saturation solubility is required for sink conditions).

Franz diffusion cells were thermoregulated at 37°C which provides a membrane temperature of 32°C (11,29). Cellulose acetate membrane (0.2 μm pore size, Sartorius, Germany) was soaked in isopropyl myristate for 2 h and mounted horizontally between the donor and receptor chambers. A volume of each emulsion equivalent to 50 μg of vitamin A was loaded to the cylindrical donor chamber and the chamber was covered with parafilm. Franz diffusion cells were fixed on a multi-position magnetic stirrer (RO 10 power IKAMAG®, IKA WERKE) and the receptor medium was continuously mixed (480±20 rpm) during the experiment. Sample aliquots of 200 μL were withdrawn from the receptor chamber at determined time intervals (1, 2, 4, 6, 8, 12, 24, 36, 48, 60, and 72 h) and replaced with fresh receptor medium. The concentration of all-*trans*-retinol in the samples was analysed with HPLC. The experimental cumulative amount of vitamin A released through the artificial membrane was determined based on Eq. 1:

$$Q = \frac{C \times V}{A} \quad (1)$$

where Q is the cumulative release per square centimeter at time t; C is the concentration of all-*trans*-retinol in the receptor phase at time t; V is the volume of the receptor compartment and A is the effective area of Franz diffusion cells (0.64±0.03 cm^2). The flux at the steady state is expressed by Eq. 2:

$$J_{ss} = \frac{C_0 KD}{L} = C_0 K_P \quad (2)$$

where C_0 is the initial concentration of the drug in the donor phase, K is the partition coefficient of the drug between the membrane and the vehicle, D is the diffusion coefficient, L is the membrane thickness and K_P is the permeability coefficient. To prevent drug loss due to photodegradation during the *in-vitro* release study, the experimental assembly was protected from light by locating in a dark room.

Skin Retention of All-trans-retinol

Experimental conditions and the apparatus for skin studies were equivalent to the above described method for *in-vitro* release studies using a synthetic membrane. The structure and thickness of porcine skin are the closest to the human skin, so due to the anatomic and physiologic similarities, the pig skin is a suitable model for skin permeability studies (30,31).

Full thickness skin from the abdominal area of large white pigs was used as an *ex-situ* skin model (Animal ethics committee approval number: 107-06, M-66-06). After removal of hair, the skin was isolated and the subcutaneous and adipose tissue was carefully removed from the excised skin. Skin samples were wrapped in aluminium foil after washing with MilliQ water and kept at −60°C to −80°C for up to 1 month after preparation. The skin integrity was assessed by measurements of electrical resistance using 4192A LF Impedance Analyzer (Hewlett Packard, MA, USA) at AC frequency of 1 kHz and pick to pick potential of 10 V with Ag/AgCl electrodes (E255, *In Vivo* Metrics, Healdsburg, CA, USA). The value of the resistance varied between 20.3 and 30.8 kΩ (skin thickness of ~0.3 cm) and was considered acceptable (32). In each run of skin retention experiments, control and silica-coated emulsions were compared using skin from the same animal to minimise the error related to skin source variation. The skin was cut into circular shaped sections (diameter: 25±5 mm) and mounted in the Franz diffusion cells with the stratum corneum in contact with the donor phase and dermis side towards the receptor medium. Great care was taken to avoid the formation of air bubbles at the interface of membrane and receptor phase. 100 μL of the emulsion was placed on the skin surface with uniform spreading and then covered with parafilm. After exposure times of 6, 12, and 24 h, skin samples were removed and the surface was rinsed three times with ethanol/water and MilliQ water respectively to eliminate the residual formulation. The excess water was absorbed with tissue; the skin was then cut

into 3×3 mm pieces. All-*trans*-retinol was extracted by acetone using sonication for 15 min under ice and then quantified with HPLC. Skin extraction as an easy and rapid quantitative method has been previously applied to quantify the *in-vitro* skin retention of 5-fluorouracil (33), caffeine (34), and retinoids (35,36). It should be noted that skin extraction yields no data on drug localization (37).

The drug concentration was also analysed in the receptor medium to determine the permeation of all-*trans*-retinol through full-thickness porcine skin after 6, 12, and 24 h treatment with control and silica-coated emulsions.

Skin Distribution of All-trans-retinol

Horizontal sectioning of skin has previously been used to characterize the distribution/localization of test compounds in skin and to generate concentration *versus* depth profiles in both *in-vivo* and *in-vitro* studies (37). We have used an equivalent method to measure the *in-vitro* skin distribution of all-*trans*-retinol. Porcine skin samples were sectioned horizontally with a Microtome/Cryostat (Miles, Tissue-Tek II) into 100-μm thick sections after treating with all-*trans*-retinol-containing control and silica-coated emulsions. The diffusion area of the skin (0.64±0.03 cm^2) was cut in a circular shape and placed in a Cryomold® (Tissue-Tek®, 15×15×5 mm) embedding in tissue freezing medium (OCT, Tissue-Tek®). Skin samples were then frozen by locating inside the Cryostat chamber (−40±3°C) and immediately sectioned. The quantity of all-*trans*-retinol was determined in individual skin sections by HPLC after the extraction process and is reported in nanograms per individual skin sections.

Skin Penetration of Silica Nanoparticles

In-vitro skin penetration of hydrophilic silica nanoparticles has been studied from an aqueous dispersion to confirm the hypothesis of the film formation and reservoir role of nanoparticles on the skin surface and simulation of the emulsions with free nanoparticles in the external water phase. Excised porcine skin samples were exposed to 0.5 wt.% aqueous dispersion of silica nanoparticles in Franz diffusion cells for up to 6 h and then vertical skin sections of 20-μm thickness were prepared using the method described previously for horizontal skin sectioning. Field Emission Scanning Electron Microscope (Philips XL30) coupled with X-ray microanalysis (EDAX Genesis V5.21) was used for imaging and elemental analysis of skin sections after coating with carbon (~15 nm). Images were taken using secondary and backscattered electron detectors at accelerating voltage of 15 kV, 3–4 μm spot size of electron beam and working distance of 10 mm. Standardless semi-quantitative X-ray analysis with ZAF corrections was performed on horizontal lines drawn along the skin depth. In addition, Inductively Coupled Plasma Atomic Emission Spectrometry (ICP-AES, Varian Australia, Pty. Ltd.) was used to determine the concentration of the ionic and atomic silica species in the receptor medium (detection limit of 0.1 μg mL^{-1}).

Statistical Analysis

Data are presented as the arithmetic mean values ±standard deviation or standard error of the mean. The test of normality using the Shapiro–Wilk test considering a 5% level of significance showed deviation from normal distribution. The statistical differences were analyzed using the non-parametric Wilcoxon rank–sum test. Two-tailed significance values ≤0.05 were considered as significant (38).

RESULTS

The Influence of Nanoparticle Layers on Physicochemical and Interfacial Emulsion Characteristics

Size distribution and zeta potential of all-*trans*-retinol-loaded oil-in-water emulsions in the absence and presence of silica nanoparticles are presented in Table I. The mean droplet size of oil-in-water emulsion without any stabilizer was 350.3±10.3 nm with polydispersity index of ~0.47 and the droplet surface was effectively uncharged (Zeta potential= −0.9±0.09 mV). The mean droplet size of the control emulsion solely stabilized with lecithin decreased from 213.3±3.2 to 171.4±2.6 and 166.5±2.1 nm by inclusion of silica nanoparticles from the oil and aqueous phases respectively. The mean droplet size of the control oleylamine emulsion (317.2±7.8 nm) reduced to 248.0±5.4 and 261.6± 6.9 nm upon the addition of silica nanoparticles to the oil and water phases.

Due to the different polar head groups in the structure of lecithin (mainly phosphatidylcholine) and oleylamine and the arrangement of these emulsifiers at the oil–water interface (39), they confer negative (−53.2±0.6 mV) and positive (+41.8±2.7 mV) charge to emulsion oil droplets, respectively. The adsorption of negatively charged silica nanoparticles (ζ potential=−25±2.5 mV (40)) at the oil–water interface has

Table I. Size Distribution and Zeta Potential of Drug-Loaded Oil-in-Water Emulsions in the Presence and Absence of Silica Nanoparticles

Emulsion	Code	Mean diameter (nm)	PI	ζ potential (mV)
Oil-in-water	O/W	350.3±10.3	0.47±0.02	−0.9±0.09
Control lecithin	L	213.3±3.2	0.23±0.01	−53.2±0.6
Lecithin+silica in oil phase	LSO	171.4±2.6	0.08±0.01	−49.9±1.9
Lecithin+silica in water phase	LSA	166.5±2.1	0.13±0.02	−52.0±1.6
Control oleylamine	O	317.2±7.8	0.51±0.04	+41.8±2.7
Oleylamine+silica in oil phase	OSO	248.0±5.4	0.32±0.03	+35.6±1.6
Oleylamine+silica in water phase	OSA	261.6±6.9	0.39±0.01	+32.0±3.9

Values are presented as the mean±SD, $n=3$

screened the positive charge of oleylamine stabilised emulsions and zeta potential has decreased to 35.6±1.6 and 32.0± 3.9 mV as a result of potential charge neutralization when nanoparticles are adsorbed at the interface from the oil and water phases respectively. Vitamin A may potentially adsorb to the interface due to the hydroxyl group in the isoprenoid side chain (25), but it has not significantly influenced the surface charge of emulsion droplets compared to drug-free emulsions. Incorporation of all-*trans*-retinol into control lecithin and oleylamine emulsions slightly increased the droplet size of drug-loaded compared to drug-free emulsions (for brevity data are not presented). No significant change in the droplet size of silica nanoparticle coated emulsions was observed due to drug incorporation.

The interfacial and bulk structure of emulsions were characterised using Freeze-Fracture SEM (Fig. 1). Smooth droplets of submicron size were observed for both control lecithin and oleylamine emulsions. Negatively charged lecithin stabilised droplets were partially coated by silica nanoparticles and the majority of particles were located in the continuous water phase (when initially added to the water phase of the emulsion) and formed a three-dimensional networks (Fig. 1, lower left). The majority of silica nanoparticles included from either oil or water phases of the emulsions containing positive oleylamine stabilised droplets were adsorbed at the interface as evidenced by partial droplet neutralisation (Table I) and further supported by EDX analysis of the droplet surface (up to 3.01 at.% silicon) in comparison to no silicon detected in the bulk.

In-vitro Active Release

Cumulative release of all-*trans*-retinol through a cellulose acetate membrane as a function of time is presented in

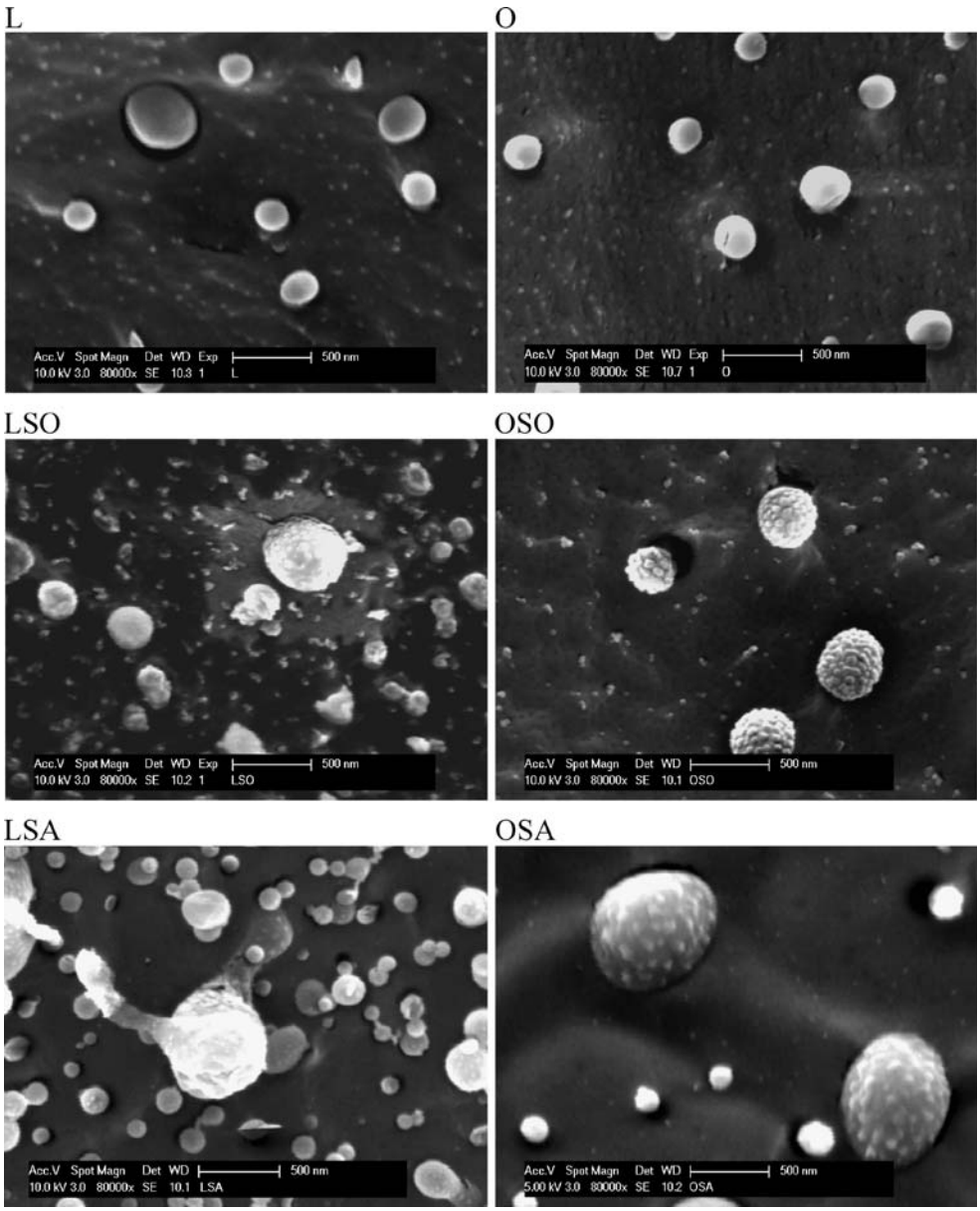

Fig. 1. Freeze-Fracture SEM images of the control and silica-coated lecithin (*left*) and oleylamine (*right*) emulsions.

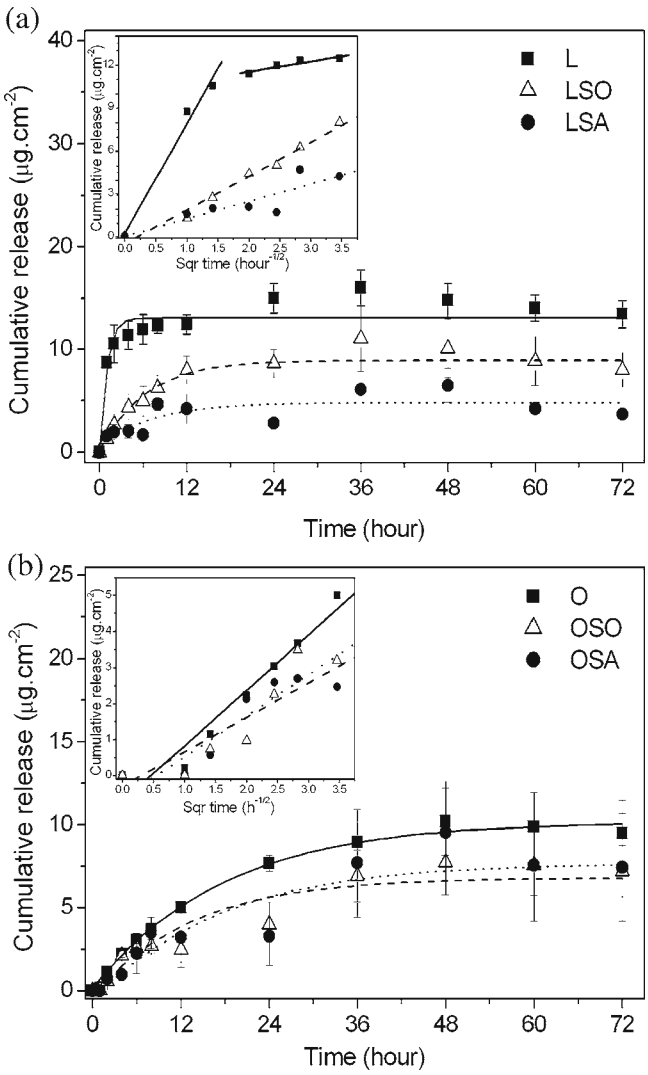

Fig. 2. *In-vitro* release of all-*trans*-retinol through cellulose acetate membrane for the control and silica-coated lecithin (**a**) and oleylamine (**b**) emulsions within 72 h (mean±SE, $n=3$). The *inset* graph shows linear fits of the release data from time 0 to 12 h against square root of time. The linear regression for the control lecithin emulsion has been depicted for a biphasic model.

Fig. 2 for the control and silica-coated lecithin (a) and oleylamine (b) emulsions. Regression analysis of the release data showed that Higuchi's model ($Q_t = K_H\sqrt{t}$) (41) was the best fit kinetic model to describe the *in-vitro* release of all-*trans*-retinol. Steady-state flux (J_{ss}) was calculated from the linear portion (t_{0h} up to t_{12h}) of the correlation between the cumulative release per unit area of the membrane and square root of time. The steady state flux, permeability coefficient, and the cumulative amount of all-*trans* retinol released within 72 h are presented in Table II.

The control lecithin emulsion showed an initial burst release followed by a slower release (Fig. 2a); the regression analysis of the cumulative release per unit area *versus* square root of time was best fitted to a biphasic model (solid lines in the insert graph in Fig. 2a). When the oil phase was the initial location of silica nanoparticles, the steady-state flux for the silica coated lecithin emulsion decreased significantly compared to the first phase (burst release) and was comparable to the release rate at the second phase of the control lecithin emulsion (1,965.6±67.5 ng cm^{-2} h$^{-1/2}$ for silica coated emulsion *vs.* 1,194.17±169.58 ng cm^{-2} h$^{-1/2}$ for control emulsion in the second phase). By inclusion of silica nanoparticles from the water phase, the value of J_{ss} (707.8±115.5 ng cm^{-2} h$^{-1/2}$) significantly reduced compared to either release phases of the control lecithin emulsion, i.e. up to ~90% reduction in the steady state flux. The cumulative release of all-*trans*-retinol over 72 h was 13.4 μg cm^{-2} for the control lecithin emulsion, which decreased to 8.0 and 3.7 μg cm^{-2} by incorporation of nanoparticles from the emulsion oil and water phases respectively.

The drug release from oleylamine emulsions showed a short lag time of 12–17 min which was not significantly different in the absence and presence of silica nanoparticles. The control oleylamine emulsion showed a slower release rate compared to the control emulsion solely stabilised with lecithin. By inclusion of nanoparticles from either phases of the control oleylamine emulsion, ~50% decrease in the steady-state flux was observed. The cumulative amount of all-*trans*-retinol released within 72 h has decreased from 9.5 μg cm^{-2} for the control oleylamine emulsion to 7.2 and 7.4 μg cm^{-2} for silica-coated emulsions.

Skin Retention of All-*trans*-Retinol

Porcine skin uptake of all-*trans*-retinol 6, 12, and 24 h after topical application of control and nanoparticle-coated lecithin and oleylamine emulsions is depicted in Fig. 3a, b. The control lecithin emulsion showed limited skin uptake; less than 0.5% of the topically applied all-*trans*-retinol was recovered in the whole skin after 24 h. Significantly higher levels of all-*trans*-retinol ($p \leq 0.05$) were detected in full-

Table II. *In-vitro* Release Characteristics of All-*trans*-Retinol Through Cellulose Acetate Membrane for Control and Silica-Coated Emulsions

Formula	Diffusional flux J_{ss} (ng cm^{-2} h$^{-1/2}$)	R^2	K_P (cm h$^{-1/2}$)	Cumulative release (μg cm^{-2}, 72 h)
L: Phase I	7,685.79±970.86	0.98	0.154±0.02	13.4±1.3
L: Phase II	1,194.17±169.58	0.94	0.024±0.003	
LSO	1,965.6±67.5	0.97	0.039±0.001	8.0±1.7
LSA	707.8±115.5	0.71	0.014±0.002	3.7±0.4
O	1,673.2±29.2	0.98	0.033±0.0006	9.5±1.9
OSO	889.4±37.6	0.94	0.018±0.0007	7.2±1.5
OSA	867.5±47.4	0.89	0.017±0.0009	7.4±1.2

Values are presented as the mean±SD, $n=3$

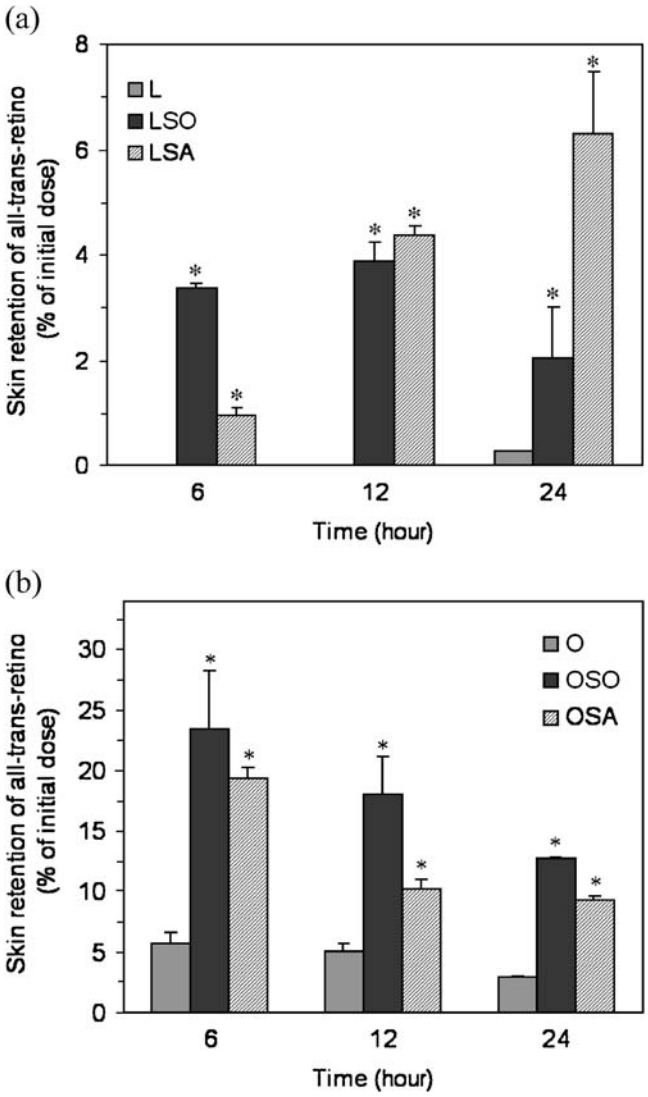

Fig. 3. Skin retention of all-*trans*-retinol from control and silica-coated lecithin (**a**) and oleylamine (**b**) stabilized emulsions. Statistical differences between the control and silica-coated emulsions were determined with Wilcoxon rank–sum test and indicated by an *asterisk* (mean±SE, $n=3$, $p \leq 0.05$).

thickness porcine skin from nanoparticle-coated in comparison to the control lecithin emulsion. In addition, the kinetics of skin uptake and transport of all-*trans*-retinol were both altered in the presence of nanoparticles. When silica nanoparticles are incorporated from the oil phase, the maximum skin uptake of all-*trans*-retinol (3.9% of the initial dose) was observed 12 h after topical application followed by the elimination of the drug from the skin which was evidenced by appearance of all-*trans*-retinol in the receptor phase after 24 h. By inclusion of nanoparticles from the aqueous phase, the dermal concentration of all-*trans*-retinol increased as a function of exposure time with a maximum skin uptake at 24 h (6.3% of the applied dose). The extent and rate of skin uptake from oleylamine emulsions were higher compared to lecithin emulsions; three to four times higher levels of all-*trans*-retinol were quantified in full-thickness skin and the maximum skin uptake was observed 6 h after topical application. Furthermore, the skin retention was significantly ($p \leq 0.05$) increased, up to four times, as a result of nanoparticle coating of oleylamine emulsion droplets.

The maximum permeation of all-*trans*-retinol through full-thickness porcine skin, i.e. the concentration detected in the receptor medium after 24 h, was 0.44% and 1.18% of the topically applied dose for lecithin and oleylamine emulsions respectively and was not significantly altered due to nanoparticle coating.

Skin Distribution of All-*trans*-Retinol

The distribution of all-*trans*-retinol as a function of porcine skin depth is demonstrated in Fig. 4 for lecithin (a) and oleylamine (b) stabilised emulsions in the absence and presence of silica nanoparticles.

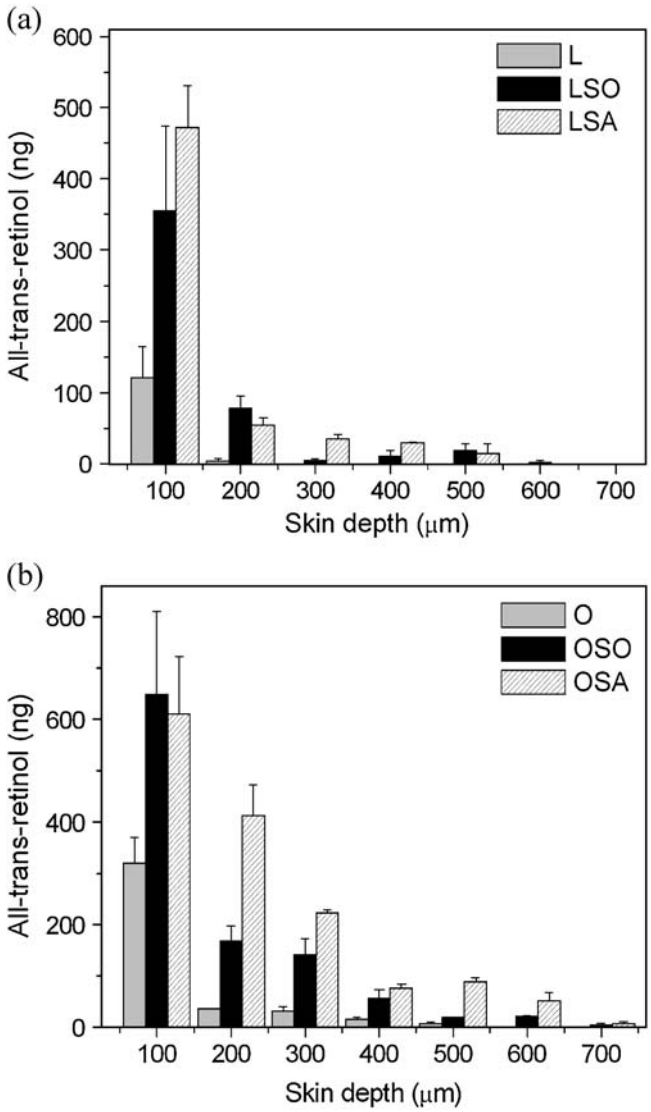

Fig. 4. Depth profile of skin distribution of all-*trans*-retinol in porcine skin after topical application of the control and silica-coated lecithin (**a**) and oleylamine (**b**) emulsions. Mean values±SE ($n=3$) of all-*trans*-retinol quantity has been reported in individual skin sections.

At skin exposure times of 6 and 12 h, due to the limited skin penetration of the control lecithin emulsion, negligible drug was detected in skin sections, and therefore the skin distribution profile was analysed using 100-μm thick skin sections after an exposure time of 24 h. This enabled us to compare the control to the silica-coated lecithin emulsions. As can be seen in Fig. 4a, after topical application of the control lecithin emulsion, ~120 ng of all-*trans*-retinol was detected in the first skin section which represents the stratum corneum and viable epidermis, with no drug could be quantified in the deeper skin slices, i.e. less than the detection limit. By silica nanoparticle inclusion from the oil or aqueous phase of the control lecithin emulsion, significantly higher amounts of all-*trans*-retinol (up to fourfold increase) was detected in the epidermis. Furthermore, all-*trans*-retinol distributed to deeper layers of skin up to a depth of 600 μm. All-*trans*-retinol quantities of ~354 and 472 ng were detected in the first 100 μm of the skin, and ~18 and ~14 ng at a depth of 500 μm when silica nanoparticles were included from the oil and aqueous phases of the control lecithin emulsion, respectively.

Silica nanoparticle coating of oleylamine-stabilised emulsion droplets also altered the distribution profile of all-*trans*-retinol; a considerably higher level of the drug was distributed to the viable epidermis and dermis (Fig. 4b). After a 24-h exposure time, all-*trans*-retinol penetrated up to a depth of 500 μm from the control oleylamine emulsion with a maximum of ~320 ng in the first 100 μm of the skin. Silica nanoparticle coating triggered deeper penetration of the drug, i.e. up to a depth of 700 μm. At a skin depth of 500 μm, only ~8 ng of all-*trans*-retinol was detected in the skin section for the control oleylamine emulsion; this increased to ~20 and ~80 ng when nanoparticles were included from the oil and aqueous phases respectively.

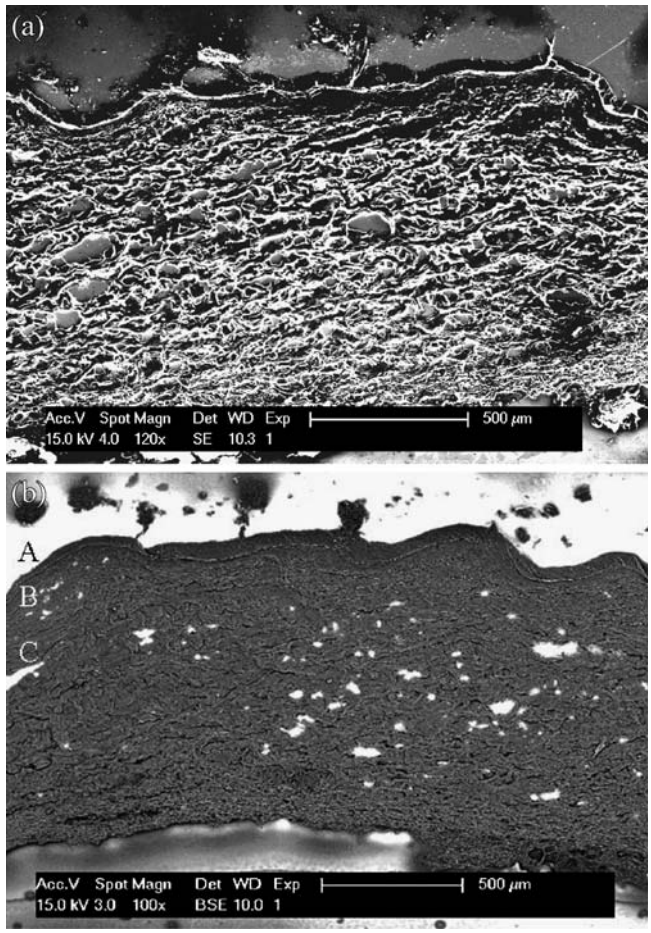

Fig. 5. Secondary (**a**) and backscattered (**b**) electron FEG-SEM image of a 20 μm-thick skin section treated with 0.5 wt.% aqueous silica dispersion. EDX analysis of horizontal lines along the skin depth showed 6.41 At % silicon at A, 3.75 At % silicon at B, and 2.55 At % silicon at C.

Skin Penetration of Silica Nanoparticles

Microscopic studies have shown that the thickness of porcine skin i.e. from the stratum corneum to the middle area of the dermis is approximately 700 μm (37). The epidermal thickness is between 30 and 140 μm and varies based on the body site (30). The secondary and backscattered electron FE-SEM images of a skin section after 6 h exposure to 0.5 wt.% silica aqueous dispersion are shown in Fig. 5. The thickness of the epidermis was between 60 and 110 μm and a film of 100–350 μm-thick of silica nanoparticles was observed on the skin surface in the backscattered electron image. Silica particles of nano-size penetrated up to the viable epidermis and upper dermis; EDX analysis of horizontal lines along the skin depth showed a decreasing trend in atomic percentage of silicon from stratum corneum towards dermis, i.e. 6.41 at.% silicon along SC, 3.75 at.% in the viable epidermis, and 2.55 at.% in the upper dermis. The permeation of silica nanoparticles through full-thickness skin i.e. the concentrations of atomic and ionic silica in the receptor phase determined by ICP-AES were 0.6±0.11 and 0.29±0.05 μg mL^{-1} respectively and were considered negligible. The skin penetration profile of silica nanoparticles from nanoparticle-coated emulsions initially stabilized with lecithin and oleylamine is under detail investigation and will be the subject of following publications.

DISCUSSION

Silica nanoparticle coating has been investigated as a novel approach to improve the physicochemical and dermal delivery characteristics of submicron oil-in-water emulsions initially stabilized with lecithin and oleylamine. The lower surface activity of oleylamine compared to lecithin at the MCT oil–water interface (22) explain the larger droplet size of oleylamine emulsions compared to lecithin emulsions. The interfacial structure of the emulsions was in good agreement with the findings of Simovic and Prestidge (21) who noted that lecithin-stabilised submicron droplets are only partially coated even in the presence of silica nanoparticle levels well above that required for multilayer formation. Partial nanoparticle coating of lecithin stabilised emulsion droplets was attributed to the weak interactions between charged nanoparticles and P–N dipole of the phospholipid head group; low oil–water interfacial tension which in turn decreases the nanoparticle attachment energy; and pronounced hydration forces.

Silica coated lecithin emulsions showed controlled release characteristics compared to the burst release observed for the control lecithin emulsion. Considering the partition coefficient value of 6.8±0.3 for all-*trans*-retinol (log PC_{oct}<9),

rapid release of the drug and lack of sustained release from conventional emulsions is predictable due to the drug partitioning (42). Washington and Evans also reported a rapid release of a probe hydrophobic drug (chlorpromazine) from lecithin-stabilised submicron triglyceride emulsions and this was attributed to the fact that commonly used emulsifiers such as lecithin do not act as a strong interfacial transport barrier (43). The observed difference in the release characteristics of lecithin and oleylamine emulsions depends on the interfacial layer structure as can be seen in Fig. 1, the initial location of nanoparticles and nanoparticle–emulsifier/drug interactions at the oil–water interface (22). The steady-state flux of silica-coated lecithin emulsions was highly dependent on the initial loading phase of nanoparticles; incorporation from the aqueous phase provided more pronounced sustained release compared to loading from the oil phase. This was due to the localization of the majority of nanoparticles in the aqueous phase in the form of three dimensional networks and accordingly potential changes in the emulsion viscosity, and the potential adsorption of all-*trans*-retinol on silica surface which may alter the distribution coefficient and release of the active agent from the emulsion carrier. The adsorption of a wide range of active agents, electrolytes, polymers, and surfactants on silica has been reported previously (44–46) and confirmed the strong adsorptive properties of silica.

On the other hand, for oleylamine emulsions, no significant effect on the release rate was observed due to the initial location of silica nanoparticles (889.4±37.6 ng cm^{-2} $h^{-1/2}$: inclusion from the oil phase *vs* 867.5±47.4 ng cm^{-2} $h^{-1/2}$: inclusion from the aqueous phase). Rabinovich-Guilatt *et al.* (39) reported that at pH_{bulk} 7.4, ~90% of oleylamine molecules were localized at the oil/water interface of medium chain triglyceride emulsions with amino groups facing the water phase. A strong electrostatic interaction between the positively charged oleylamine and negatively charged silica nanoparticles resulted in the favorable attachment of silica nanoparticles at the oil–water interface regardless of their initial location as confirmed by Freeze-Fracture SEM (Fig. 1) and decreased zeta potential values of the resultant emulsions (Table I). The interfacial complex formed as a result of synergistic interaction between oleylamine and silica nanoparticles acted as a barrier for the transport of all-*trans*-retinol, and considering the similar interfacial arrangement by incorporation of nanoparticles from the oil or aqueous phase of the emulsion, the sustained release effect was equivalent (Table II). Release kinetics of a poorly soluble lipophilic molecule (di-butyl-phtalate) from polydimethylsiloxane droplets in water and influence of silica nanoparticle layers have been reported by Simovic and Prestidge (15). A correlation was established between the interfacial structure of nanoparticle layers at emulsion droplet surface and the drug release rate. Significant sustained release was achieved by rigid multilayers of hydrophobised silica nanoparticles at the oil–water interface.

The skin retention of all-*trans*-retinol was also dependent on the initial emulsifier type and was three to four times higher from positively charged oleylamine compared to negatively charged lecithin droplets. Similarly, Montenegro *et al.* (8) reported significantly higher retinoic acid skin penetration from positively charged compared to neutral or negatively charged liposomes. This was attributed to the greater accumulation of these liposomes within the stratum corneum due to the electrostatic attraction to the negative charge of the skin surface. The isoelectric point of the skin is between 3.5 and 4.8, hence the skin is negatively charged under physiological conditions (47,48). The higher skin uptake of all-*trans*-retinol in the presence of oleylamine in this study can also be related to the perturbation in the lipid structure of the stratum corneum; this has been demonstrated by the frequency alterations in the CH–asymmetric stretching band near 2,920 cm^{-1} in the stratum corneum analysed with FT-IR/ATR (Fourier transform infrared/attenuated total reflection) (49).

Increased skin accumulation and simultaneously decreased permeation through the skin has been previously reported for a range of active agents from lipidic and polymeric nanoparticles (7,11,50–54). The negligible permeation through the full-thickness porcine skin, in parallel to the significant increase in the skin retention of all-*trans*-retinol in this study confirmed the suitability of silica nanoparticle-coated submicron emulsions for topical delivery of this lipophilic molecule. The improvement in the dermal delivery of active agents due to the nanoparticles has been related to a number of different mechanisms such as changes in the solubility parameter of the skin and accordingly the drug partitioning into the skin (55), the increased thermodynamic activity of the drug (56), and alteration of the skin hydration (57–60) and barrier function (61). Based on the existing hypotheses and our findings regarding the physicochemical and interfacial characteristics of nanoparticle-coated emulsions, the following mechanisms are proposed for the observed improvement in the dermal delivery of all-*trans*-retinol from these specific vehicles.

Improved Physical Stability of the Emulsion Carrier and Chemical Stability of the Active Agent

Silica nanoparticle coating of drug-free medium chain triglyceride oil-in-water emulsions stabilized with lecithin and oleylamine resulted in improved emulsification efficiency and long-term stability towards coalescence and creaming (22). The formation and stability of the emulsions were correlated to the interfacial interactions between charged droplets and hydrophilic silica nanoparticles which resulted in the partial coverage of negatively charged lecithin droplets but strong electrostatic coating of positively charged oleylamine droplets (Fig. 1). However, the composition of the topical formulation rarely remains constant after application on the skin surface; water evaporates and emulsions form a thin film on the skin surface. The mobility and distribution coefficient of the active agent changes as a function of its concentration and the viscosity and phase behavior of the topical vehicle (62). The more significant influence of silica nanoparticles on the rate and extent of skin retention when nanoparticles are present in the aqueous phase compared to the oil phase of the control lecithin emulsion is considered to be due to nanoparticle networks in the external water phase (Fig. 1, lower left) which in turn changes the viscosity (63–66) and evaporation of water from the emulsion.

In addition, submicron size emulsion oil droplets in the silica-coated emulsions with improved stability and integrity would likely penetrate the skin more efficiently than larger or coalesced droplets in the case of the control emulsions (29). The improvement in the chemical stability of all-*trans*-retinol

as a result of silica nanoparticle coating is under detail investigation as another potential mechanism for the improved dermal delivery characteristics.

Nanoparticle–Skin Interactions

EDX analysis of the layer on skin surface in the backscattered FEG-SEM image of skin section treated with 0.5 wt.% aqueous silica dispersion (Fig. 5) confirmed a high intensity of silica and accumulation of nanoparticles in the form of a thick film on the skin surface. The formation of a semisolid film composed of emulsion oil droplets as well as a silica nanoparticle layer on the skin surface may contribute to the increased skin occlusion. Similarly, the film formation model of Müller and Dingler (57) described the occlusive effect of nanosize particles on the skin; the evaporation of water from the skin surface is hydrodynamically unfavorable due to the high coverage by a hexagonal packed monolayer of nanoparticles. As a result, the skin hydration increases and penetration of the active ingredient is promoted (58,60). In addition, this film on the skin surface can serve as a reservoir for all-*trans*-retinol associated/adsorbed on silica nanoparticles or in the emulsion oil droplets and the active agent can diffuse to deeper layers of skin through the more hydrated stratum corneum. Microscopic images of porcine skin treated with a SLN-containing cream confirmed the occlusive effect of solid lipid nanoparticles based on the significant changes in the thickness and shape of the stratum corneum (59). The high specific surface area of nanometre-sized silica particles may also contribute to targeted dermal delivery by facilitating the contact of the encapsulated molecule with the stratum corneum (7). Baroli *et al.* (61) also reported the penetration and formation of intercellular deposits of metallic nanoparticles within the stratum corneum. Nanoparticles were able to passively penetrate the skin reaching the viable epidermis without permeation through the skin. This was partly attributed to the alteration of the lipid matrix organization and skin resistivity due to nanoparticles.

Jenning *et al.* (11) reported a retinol localising effect to the upper skin layers which was limited to a few hours due to the polymorphic transition and drug expulsion from solid lipid nanoparticles. The presence of specific lipids in the composition of SLN has been shown to improve the targeting behavior, but in addition, a close association/interaction of the drug molecule and the carrier was considered critical for drug targeting effect (67). Puglia *et al.* (50) also reported significantly higher concentrations of ketoprofen and naproxen loaded into NLC (nanostructured lipid carriers) compared to free drug in the stratum corneum using a tape stripping method. The lipid bioadhesive properties and the formation of the reservoir on the skin surface were partly responsible for the observed effect, although the exact mechanism was unclear. The results of this study confirmed the potential of nanoparticle-coated submicron emulsions as vehicles of all-*trans*-retinol with improved dermal delivery characteristics.

In the light of recent toxicological risk assessment that showed small nanoparticles below 10 nm can penetrate through the stratum corneum lipidic matrix and hair follicle orifices and reach up to the viable epidermis without permeation through full-thickness human skin (61,68), we may comment that our porcine skin study can be a useful guidance. However, for assessment of potential toxicological risks of the proposed formulations, human skin toxicological response studies have to be conducted; this is outside the scope of the current article. In addition, nature of nanoparticle materials plays an important role in human skin toxicological response. Considering that hydrophilic silica materials are recently proposed for implants and their biocompatibility has been proven (69), it is reasonable to consider that skin biocompatibility might be acceptable. Oral and topical toxicity data on cosmetic preparations or sunscreens showed that TiO_2 and ZnO (~30 nm) nanoparticles have low systemic toxicity and are limited to the outer surface of the human stratum corneum with no particles detected in the lower stratum corneum or viable epidermis (32,70). The skin permeation and accordingly the systemic exposure of topically applied nanoparticles have been of great importance due to the potential pro-inflammatory and cytotoxicity effect (32). The effect of nano-scaled SiO_2 particles on endothelial cell function and viability has been evaluated. Exposure of human endothelial cells to different amounts of the particles showed the internalisation of silica nanoparticles with no cytotoxic effect. But an impairment of the proliferative activity and a pro-inflammatory stimulation of endothelial cells (suggesting a possible *in-vivo* chronic inflammation) were induced by exposure to SiO_2 particles of nano-size (71).

CONCLUSION

Silica nanoparticle coating of medium chain triglyceride oil-in-water emulsions results in sustained *in-vitro* release of all-*trans*-retinol. The initial emulsifier (lecithin/oleylamine) and the loading phase of nanoparticles played an important role in the *in-vitro* release kinetics, skin penetration and distribution. Significantly higher skin uptake of all-*trans*-retinol was observed from nanoparticle-coated emulsions compared to the control emulsions. The distribution profile of all-*trans*-retinol indicated the drug localization in the upper skin layers and deeper penetration up to the viable epidermis and upper dermis. The permeation of all-*trans*-retinol through full-thickness porcine skin was negligible from the investigated carriers. This investigation demonstrated that silica nanoparticles can control the *in-vitro* release and promote skin retention of all-*trans* retinol in emulsion-based topical pharmaceutical preparations. Silica nanoparticles facilitated accumulation of all-*trans* retinol in target skin layers due to the improved characteristics of the emulsion carrier and modified skin hydration and barrier function. These emulsion based hybrid drug delivery systems showed improved topical delivery of all-*trans*-retinol; nanoparticle layers significantly improved the performance of O/W emulsions as encapsulation and delivery systems for all-*trans*-retinol.

ACKNOWLEDGEMENT

The Australian Research Council's Discovery grant scheme (DP0558920), Itek Pty. Ltd., and BioInnovation SA are acknowledged for the funding. The authors thank Dr. Peter Self for the assistance with the Freeze-Fracture SEM.

REFERENCES

1. De Luca LM, Shapiro SS (eds). Modulation of cellular interactions by vitamin A and derivatives (retinoids). New York: New York Academy of Sciences; 1981.
2. Dawson MI, Okamura WH. Chemistry and biology of synthetic retinoids. Boca Raton: CRC; 1990.
3. Koizumi Y. Effect of retinoids on the skin diseases. Fragrance J Jpn 1992;20:26–31.
4. Szuts EZ, Harosi FI. Solubility of retinoids in water. Arch Biochem Biophys 1991;287:297–304. doi:10.1016/0003-9861(91)90482-X.
5. Lee S-C, Yuk H-G, Lee D-H, Lee K-E, Hwang Y-I, Ludescher RD. Stabilization of retinol through incorporation into liposomes. J Biochem Mol Biol 2002;35:358–63.
6. Shefer A, Shefer SD. Stabilised retinol for cosmetic dermatological, and pharmaceutical compositions, and use thereof. US Pat., WO 03/105806 A1, 2003.
7. Alvarez Román R, Naik A, Kalia YN, Guy RH, Fessi H. Enhancement of topical delivery from biodegradable nanoparticles. Pharm Res 2004;21:1818–25. doi:10.1023/B:PHAM.0000045235.86197.ef.
8. Montenegro L, Panico AM, Ventimiglia A, Bonina FP. *In vitro* retinoic acid release and skin permeation from different liposome formulations. Int J Pharm 1996;133:89–96. doi:10.1016/0378-5173(95)04422-1.
9. Lee M-H, Oh S-G, Moon S-K, Bae S-Y. Preparation of silica particles encapsulating retinol using O/W/O multiple emulsions. J Colloid Interface Sci 2001;240:83–9. doi:10.1006/jcis.2001.7699.
10. Weisse S, Perly B, Dalbiez J-P, Baraton-Ouvrard F, Archambault J-C, Andre P, *et al*. New aqueous gel based on soluble cyclodextrin/vitamin A inclusion complex. J Incl Phenom Macrocycl Chem 2002;44:87–91. doi:10.1023/A:1023084900159.
11. Jenning V, Gysler A, Schafer-Korting M, Gohla SH. Vitamin A loaded solid lipid nanoparticles for topical use: occlusive properties and drug targeting to the upper skin. Eur J Pharm Biopharm 2000;49:211–8. doi:10.1016/S0939-6411(99)00075-2.
12. Jenning V, Schafer-Korting M, Gohla S. Vitamin A-loaded solid lipid nanoparticles for topical use: drug release properties. J Control Release 2000;66:115–26. doi:10.1016/S0168-3659(99)00223-0.
13. Torrado S, Torrado JJ, Cadorniga R. Topical application of albumin microspheres containing vitamin A: drug release and availability. Int J Pharm 1992;86:147–52. doi:10.1016/0378-5173(92)90191-4.
14. Swatschek D, Schatton W, Müller WEG, Kreuter J. Microparticles derived from marine sponge collagen (SCMPs): preparation, characterization and suitability for dermal delivery of all-trans retinol. Eur J Pharm Biopharm 2002;54:125–33. doi:10.1016/S0939-6411(02)00046-2.
15. Simovic S, Prestidge CA. Nanoparticle layers controlling drug release from emulsions. Eur J Pharm Biopharm 2007;67:39–47. doi:10.1016/j.ejpb.2007.01.011.
16. Binks BP, Lumsdon SO. Influence of particle wettability on the type and stability of surfactant-free emulsions. Langmuir 2000;16:8622–31. doi:10.1021/la000189s.
17. Binks BP, Whitby CP. Nanoparticle silica-stabilised oil-in-water emulsions: improving emulsion stability. Colloids Surf A 2005;253:105–15. doi:10.1016/j.colsurfa.2004.10.116.
18. Binks BP, Rodrigues JA, Frith WJ. Synergistic interaction in emulsions stabilized by a mixture of silica nanoparticles and cationic surfactant. Langmuir 2007;23:3626–36. doi:10.1021/la0634600.
19. Lan Q, Yang F, Zhang S, Liu S, Xu J, Sun D. Synergistic effect of silica nanoparticle and cetyltrimethyl ammonium bromide on the stabilization of O/W emulsions. Colloids Surf A 2007;302:126–35. doi:10.1016/j.colsurfa.2007.02.010.
20. Simovic S, Prestidge CA. Adsorption of hydrophobic silica nanoparticles at the PDMS droplet-water interface. Langmuir 2003;19:8364–70. doi:10.1021/la0347197.
21. Simovic S, Prestidge CA. Colloidosomes from controlled interaction of submicrometer triglyseride droplets and hydrophilic silica nanoparticles. Langmuir 2008;24:7132–7. doi:10.1021/la800862v.
22. Ghouchi-Eskandar N, Simovic S, Prestidge CA. Synergistic effect of silica nanoparticles and charged surfactants in the formation and stability of submicron oil-in-water emulsions. Phys Chem Chem Phys 2007;9:6426–34. doi:10.1039/b710256a.
23. Technical Bulletin Pigments, Evonik Degussa GmbH, Hanau. http://www.degussa.com (1994).
24. Yan N, Maham Y, Masliyah JH, Gray MR, Mather AE. Measurement of contact angles for fumed silica nanospheres using enthalpy of immersion data. J Colloid Interface Sci 2000;228:1–6. doi:10.1006/jcis.2000.6856.
25. Washington C. Stability of lipid emulsions for drug delivery. Adv Drug Deliv Rev 1996;20:131–45. doi:10.1016/0169-409X(95)00116-O.
26. Jenning V, Gohla SH. Encapsulation of retinoids in solid lipid nanoparticles (SLN®). J Microencapsul 2001;18:149–58. doi:10.1080/02652040010000361.
27. Moren M, Gundersen TE, Hamre K. Quantitative and qualitative analysis of retinoids in Artemia and copepods by HPLC and diode array detection. Aquaculture 2005;246:359–65. doi:10.1016/j.aquaculture.2005.01.017.
28. Stancher B, Zonta F. Comparison between straight and reversed phases in the high-performance liquid chromatographic fractionation of retinol isomers. J Chromatogr A 1982;234:244–8. doi:10.1016/S0021-9673(00)81802-6.
29. Amselem S, Friedman D. Submicron emulsions as drug carriers for topical administration. In: Benita S, editor. Submicron emulsions in drug targeting and delivery. London: Harwood Academic; 1998. p. 153–73.
30. Sullivan TP, Eaglstein WH, Davis SC, Mertz P. The pig as a model for human wound healing. Wound Repair Regen 2001;9:66–76. doi:10.1046/j.1524-475x.2001.00066.x.
31. Bronaugh RL, Stewart RF, Congdon ER. Methods for *in vitro* percutaneous absorption studies II. Animal models for human skin. Toxicol Appl Pharmacol 1982;62:481–8. doi:10.1016/0041-008X(82)90149-1.
32. Cross SE, Innes B, Roberts MS, Tsuzuki T, Robertson TA, McCormick P. Human skin penetration of sunscreen nanoparticles: *in-vitro* assessment of a novel micronized zinc oxide formulation. Skin Pharmacol Physiol 2007;20:148–54. doi:10.1159/000098701.
33. Touitou E, Abed L. Effect of propylene glycol, azone and n-decylmethyl sulphoxide on skin permeation kinetics of 5-fluorouracil. Int J Pharm 1985;27:89–98. doi:10.1016/0378-5173(85)90188-7.
34. Touitou E, Levi-Schaffer F, Dayan N, Alhaique F, Riccieri F. Modulation of caffeine skin delivery by carrier design: liposomes *versus* permeation enhancers. Int J Pharm 1994;103:131–6. doi:10.1016/0378-5173(94)90093-0.
35. Lehman PA, Slattery JT, Franz TJ. Percutaneous absorption of retinoids: influence of vehicle, light exposure, and dose. J Invest Dermatol 1988;91:56–61. doi:10.1111/1523-1747.ep12463289.
36. Lehman PA, Malany AM. Evidence for percutaneous absorption of isotretinoin from the photo-isomerization of topical tretinoin. J Invest Dermatol 1989;93:595–9. doi:10.1111/1523-1747.ep12319721.
37. Touitou E, Meidan VM, Horwitz E. Methods for quantitative determination of drug localized in the skin. J Control Release 1998;56:7–21. doi:10.1016/S0168-3659(98)00060-1.
38. Field A. Discovering statistics using SPSS. 2nd ed. London: Sage; 2005.
39. Rabinovich-Guilatt L, Couvreur P, Lambert G, Goldstein D, Benita S, Dubernet C. Extensive surface studies help to analyse zeta potential data: the case of cationic emulsions. Chem Phys Lipids 2004;131:1–13. doi:10.1016/j.chemphyslip.2004.04.003.
40. Simovic S, Prestidge CA. Hydrophilic silica nanoparticles at the PDMS droplet-water interface. Langmuir 2003;19:3785–92. doi:10.1021/la026803c.
41. Costa P, Sousa Lobo JM. Modeling and comparison of dissolution profiles. Eur J Pharm Sci 2001;13:123–33. doi:10.1016/S0928-0987(01)00095-1.
42. Nishikawa M, Takakura Y, Hashida M. Biofate of fat emulsions. In: Benita S, editor. Submicron emulsions in drug targeting and delivery. London: Harwood Academic; 1998. p. 99–118.

43. Washington C, Evans K. Release rate measurements of model hydrophobic solutes from submicron triglyceride emulsions. J Control Release 1995;33:383–90. doi:10.1016/0168-3659(94)00110-G.
44. Sanganwar GP, Gupta RB. Dissolution-rate enhancement of fenofibrate by adsorption onto silica using supercritical carbon dioxide. Int J Pharm 2008;360:213–8. doi:10.1016/j.ijpharm.2008.04.041.
45. Golub TP, Koopal LK, Sidorova MP. Adsorption of cationic surfactants on silica surface: 1. adsorption isotherms and surface charge. Colloid J 2004;66:38–43. doi:10.1023/B:COLL.0000015053.71438.fd.
46. Sobisch T. On the adsorption of polyoxyethylene p-tert-octylphenyl ether on silica. Colloids Surf 1992;66:11–21. doi:10.1016/0166-6622(92)80116-J.
47. Wilkerson VA. The chemistry of human epidermis II. The isoelectric point of the stratum corneum, hair, and nails as determined by electrophoresis. J Biol Chem 1935;112:329–35.
48. Higaki K, Amnuaikit C, Kimura T. Strategies for overcoming the stratum corneum: chemical and physical approaches. Am J Drug Deliv 2003;1:187–214. doi:10.2165/00137696-200301030-00004.
49. Takeuchi Y, Yasukawa H, Yamaoka Y, Moromoto Y, Nakao S, Fukumori Y, *et al*. Destabilization of whole skin lipid bioliposomes induced by skin penetration enhancers and FT-IR/ATR (Fourier transform infrared/attenuated total reflection) analysis of stratum corneum lipids. Chem Pharm Bull 1992;40:484–7.
50. Puglia C, Blasi P, Rizza L, Schoubben A, Bonina F, Rossi C, *et al*. Lipid nanoparticles for prolonged topical delivery: an *in vitro* and *in vivo* investigation. Int J Pharm 2008;357:295–304. doi:10.1016/j.ijpharm.2008.01.045.
51. Liu J, Hu W, Chen H, Ni Q, Xu H, Yang X. Isotretinoin-loaded solid lipid nanoparticles with skin targeting for topical delivery. Int J Pharm 2007;328:191–5. doi:10.1016/j.ijpharm.2006.08.007.
52. Chen H, Chang X, Du D, Liu W, Liu J, Weng T, *et al*. Podophyllotoxin-loaded solid lipid nanoparticles for epidermal targeting. J Control Release 2006;110:296–306. doi:10.1016/j.jconrel.2005.09.052.
53. Lombardi Borgia S, Regehly M, Sivaramakrishnan R, Mehnert W, Korting HC, Danker K, *et al*. Lipid nanoparticles for skin penetration enhancement-correlation to drug localization within the particle matrix as determined by fluorescence and parelectric spectroscopy. J Control Release 2005;110:151–63. doi:10.1016/j.jconrel.2005.09.045.
54. de Jalón EG, Blanco-Príeto MJ, Ygartua P, Santoyo S. Topical application of acyclovir-loaded microparticles: quantification of the drug in porcine skin layers. J Control Release 2001;75:191–7. doi:10.1016/S0168-3659(01)00395-9.
55. Hadgraft J. Skin, the final frontier. Int J Pharm 2001;224:1–18. doi:10.1016/S0378-5173(01)00731-1.
56. Cho SH, Kim SY, Lee SI, Lee YM. Hydroxypropyl-ß-cyclodextrin inclusion complexes for transdermal delivery: preparation, inclusion properties, stability, and release behavior. J Ind Eng Chem 2006;12:50–9.
57. Müller RH, Dingler A. The next generation after the liposomes: solid lipid nanoparticles as dermal carrier in cosmetics. Eurocosmetics 1998;7–8:19–26.
58. Müller RH, Radtke M, Wissing SA. Solid lipid nanoparticles (SLN) and nanostructured lipid carriers (NLC) in cosmetic and dermatological preparations. Adv Drug Deliv Rev 2002;54:S131–55. doi:10.1016/S0169-409X(02)00118-7.
59. Müller RH, Mäder K, Gohla S. Solid lipid nanoparticles (SLN) for controlled drug delivery—a review of the state of the art. Eur J Pharm Biopharm 2000;50:161–77. doi:10.1016/S0939-6411(00)00087-4.
60. Dingler A, Blum RP, Neihus H, Müller RH, Gohla S. Solid lipid nanoparticles (SLN™/Lipopearls™)—a pharmaceutical and cosmetic carrier for the application of vitamin E in dermal products. J Microencapsul 1999;16:751–67. doi:10.1080/026520499288690.
61. Baroli B, Ennas MG, Loffredo F, Isola M, Pinna R, Lopez-Quintela MA. Penetration of metallic nanoparticles in human full-thickness skin. J Invest Dermatol 2007;127:1701–12.
62. Binks BP, editor. Modern aspects of emulsion science. Cambridge: The Royal Society of Chemistry; 1998.
63. Thieme J, Abend S, Lagaly G. Aggregation in Pickering emulsions. Colloid Polym Sci 1999;277:257–60. doi:10.1007/PL00013752.
64. Levine S, Bowen BD, Partridge SJ. Stabilization of emulsions by fine particles I. Partitioning of particles between continuous phase and oil/water interface. Colloids Surf 1989;38:325–43. doi:10.1016/0166-6622(89)80271-9.
65. Yan Y, Masliyah JH. Solids-stabilized oil-in-water emulsions: scavenging of emulsion droplets by fresh oil addition. Colloids Surf A 1993;75:123–32. doi:10.1016/0927-7757(93)80423-C.
66. Abend S, Lagaly G. Bentonite and double hydroxides as emulsifying agents. Clay Miner 2001;36:557–70. doi:10.1180/0009855013640009.
67. Sivaramakrishnan R, Nakamura C, Mehnert W, Korting HC, Kramer KD, Schäfer-Korting M. Glucocorticoid entrapment into lipid carriers—characterisation by parelectric spectroscopy and influence on dermal uptake. J Control Release 2004;97:493–502.
68. Baroli B. Nanoparticles and skin penetration. Are there any potential toxicological risks? J Verbr Lebensm 2008;3:330–1.
69. Vallet-Regi M, Balas F, Arcos D. Mesoporous materials for drug delivery. Angew Chem Int Ed 2007;46:7548–58. doi:10.1002/anie.200604488.
70. Nohynek GJ, Lademann Jr, Ribaud C, Roberts MS. Grey Goo on the skin? Nanotechnology, cosmetic and sunscreen safety. Crit Rev Toxicol 2007;37:251–77. doi:10.1080/10408440601177780.
71. Peters K, Unger RE, Kirkpatrick CJ, Gatti AM, Monari E. Effects of nano-scaled particles on endothelial cell function *in vitro*: studies on viability, proliferation and inflammation. J Mater Sci Mater Med 2004;15:321–5. doi:10.1023/B:JMSM.0000021095.36878.1b.